EPJ manuscript No.
(will be inserted by the editor)

FZJ–IKP(TH)–2007–07

The $\mathrm{pp}\to\mathrm{K}^+\Sigma^+\mathrm{n}$ cross section from missing mass spectra

A. Sibirtsev[1], J. Haidenbauer[2], H.-W. Hammer[1] and Ulf-G. Meißner[1,2]

[1] Helmholtz-Institut für Strahlen- und Kernphysik (Theorie), Universität Bonn, Nußallee 14-16, D-53115 Bonn, Germany
[2] Institut für Kernphysik, Forschungszentrum Jülich, D-52425 Jülich, Germany

the date of receipt and acceptance should be inserted later

Abstract. We utilize existing inclusive data on K^+-meson momentum spectra of the reaction $pp\to K^+X$ at T_p = 2.3 - 2.85 GeV to deduce total cross sections for $pp\to K^+\Sigma^+n$. The method used to extract those cross sections is explained and discussed in detail. Our result for T_p = 2.85 GeV is consistent with the data point from a direct measurement at the same beam energy. The cross section obtained for T_p = 2.3 GeV is with 13.7 ± 2.3 μb considerably smaller than the value found in a recent experiment by the COSY-11 Collaboration at a somewhat lower beam energy, indicating that the $pp\to K^+\Sigma^+n$ reaction cross section could exhibit a rather unusual energy dependence.

PACS. 13.75.Ev Hyperon-nucleon interactions – 13.75.Jz Kaon-baryon interactions – 14.20.Gk Baryon resonances with S=0 – 25.40.Ny Resonance reactions

1 Introduction

Recently first near-threshold cross section data for the $pp \to K^+\Sigma^+n$ reaction were published by the COSY-11 Collaboration [1]. Surprisingly, it turned out that this cross section is larger than the one for $pp\to K^+\Sigma^0p$ by a factor of around 230 at the excess energy ϵ=13 MeV and by a factor of around 90 at ϵ=60 MeV. The excess energy ϵ is defined as $\epsilon=\sqrt{s}-m_K-m_\Sigma-m_N$, where s is the squared invariant collision energy, while m_K, m_Σ and m_N are the masses of the kaon, the Σ hyperon and the nucleon, respectively. It is also worth mentioning that none of the available model calculations [2,3,4,5,6] is able to describe those data. In fact, most of those models underestimate the cross section by an order of magnitude or even more.

Besides this rather large value for the production cross section as compared to the Σ^0p channel, the new results for the $pp\to K^+\Sigma^+n$ reaction are also somewhat startling when compared with the available high energy data. Indeed, one can find only five data points [7,8,9,10] for $pp\to K^+\Sigma^+n$ at higher energies in the literature. Moreover, those data show large fluctuations, even considering the large experimental uncertainties, and two of those points [9] were reported only in a preprint. But it is still obvious that the COSY-11 result at ϵ=60 MeV [1] is as large as the $pp\to K^+\Sigma^+n$ cross section measured at higher energies [7,8,10], suggesting that there could be practically no energy dependence over the large energy region $60\leq\epsilon\leq1000$ MeV with the mean cross section being 49 ± 5 μb. That is a rather unexpected result since the cross section of $pp\to K^+\Sigma^0p$, the only well investigated Σ production channel, shows a significant energy dependence, as expected from the increasing phase space for the reaction. Indeed here the cross section changes by a factor of about 40 within the energy range indicated above.

The data points [7,8,9,10] at high energies are obtained from bubble chamber images where the identification of the $pp \to K^+\Sigma^+n$ as well as the $pp\to K^+\Sigma^0p$ reaction channel was done simultaneously and unambiguously. Therefore, these results at high energies might be fairly reliable. The situation with regard to the more recent counter experiments is different. Here the $pp\to K^+\Sigma^+n$ channel was often not considered because of the substantial difficulties in the final particle identification. The COSY-11 collaboration reconstructs the kaon and neutron four-momenta and identifies the Σ^+-hyperon by the missing mass. It was found [1] that the large background under the Σ^+-signal complicates the data analysis considerably and it introduces large uncertainties. A much better, i.e. direct, identification of the Σ^+ can be done by detecting the $\Sigma^+\to p\pi^0$ decay mode, though then a photon detector is required. Indeed, a corresponding experiment has been already proposed [11] for the WASA detector [12] at the COSY facility.

With the present paper we want to supply some more values for the $pp\to K^+\Sigma^+n$ cross section to the data base. For that aim we utilize available data on inclusive K^+-meson momentum spectra measured at different angles in pp collisions for the reaction $pp\to K^+X$. Since the experimental K^+-meson momentum spectra [13,14,15] are available at energies that lie between the data of the COSY-11 Collaboration and the high energy data, the result of our analyis allows conclusions on the behavior of the $pp\to K^+\Sigma^+n$ cross section in this interesting energy region. Some of the spectra are available at energies that overlap with the bubble chamber results [7] and, therefore, we can also check whether the results based on our method are compatible with the high energy measurement. As a byproduct we also provide cross sections for the $pp\to K^+\Lambda p$ reaction and compare them with direct measurements, where the latter are based on the reconstruction of the final particles.

The paper is organized as follows: In Sec. 2 we describe the method. The analysis of the data is presented in Sec. 3. Our results are compared to other available data in Sec. 4. The paper ends with a short summary.

2 Method for the data evaluation

In this section we describe in detail the method for the data analysis. For completeness we include all relevant formulas, although some of them are given in Ref. [16]. Furthermore, since this method is not limited specifically to $pp\to K^+\Sigma^+n$ but applicable to any reaction with a three-body final state, we provide the formalism in a general form. The cross section for the $a+b\to 1+2+3$ reaction is given by

$$\sigma=\frac{1}{2^6\pi^5\lambda^{1/2}(s,m_a^2,m_b^2)}\int\frac{d^3p_1}{2E_1}\,\frac{d^3p_2}{2E_2}\,\frac{d^3p_3}{2E_3} \times\delta(P_1+P_2+P_3-P_a-P_b)\,|\mathcal{A}|^2\,, \qquad (1)$$

where p_i and E_i are the 3-momentum and the energy of the i-th particle, respectively, while P_i stands for the 4-momentum. $\mathcal{A}$ denotes the reaction amplitude and the λ-function is defined by $\lambda(x,y,z)=(x-y-z)^2-4yz$. We use the invariants

$$s=P^2=(P_a+P_b)^2,\quad s_Q=Q^2=(P_2+P_3)^2=(P-P_1)^2, \qquad (2)$$

where s_Q is the squared missing mass with respect to the first particle, which is identical to the squared invariant mass of the second and third particle. The Lorentz invariant differential cross section for the production of particle 1 is then written as

$$\frac{E_1}{p_1^2}\frac{d^3\sigma}{dp_1d\Omega_1}=\frac{1}{2^7\pi^5\lambda^{1/2}(s,m_a^2,m_b^2)}\int\frac{d^3p_2}{2E_2}\,\frac{d^3p_3}{2E_3} \times\delta(P_2+P_3-Q)\;|\mathcal{A}|^2=\frac{1}{2^8\pi^4\lambda^{1/2}(s,m_a^2,m_b^2)} \times\frac{\lambda^{1/2}(s_Q,m_2^2,m_3^2)}{s_Q}\;\overline{|\mathcal{A}|^2}\,. \qquad (3)$$

In the laboratory frame, i.e. for $P_b=(\mathbf{0},m_b)$, s_Q can be expressed as

$$s_Q=s+m_1^2-2(E_a+m_b)E_1+2p_ap_1cos\theta_1, \qquad (4)$$

where Ω_1 and θ_1 are the solid and polar production angle of the first particle. In Eq. (3), $\overline{|\mathcal{A}|^2}$ is the square of the reaction amplitude integrated over the kinematical variables related to the second and third particle. In general $\overline{|\mathcal{A}|^2}$ depends on p_1 (or s_Q), $\Omega_1=(\theta_1,\phi_1)$ and s.

The relation between the differential momentum spectrum measured at the solid angle Ω_1 and the missing mass (M_X) spectrum, where $M_X^2=s_Q$, is given by

$$\frac{d^3\sigma}{dM_Xd\Omega_1}=\sqrt{s_Q}\,\left[\frac{E_a+m_b}{\sqrt{p_1^2+m_1^2}}\,p_1-p_a\cos\theta_1\right]^{-1}\frac{d^3\sigma}{dp_1d\Omega_1}\,. \qquad (5)$$

In order to exemplify how we proceed in our analysis let us consider here two typical data samples for the $pp\to K^+X$ reaction. One is from a measurement at the beam energy T_p=2.3 GeV and the K^+-production angle $\theta_K=10.3^o$ [14] and the other at T_p=2.54 GeV and $\theta_K=30^o$ [13]. Both data sets are shown in Fig. 1, where the left panel illustrates the K^+-meson momentum spectra, while the right panel shows the missing mass spectra obtained by Eq. (5). The arrows in Fig. 1 indicate the $K\Sigma N$ and $K\Lambda N\pi$ reaction thresholds, respectively. Below the $K\Sigma N$ threshold, i.e. for $M_X\leq m_\Sigma+m_N$, kaon production is primarily due to the $pp\to K^+\Lambda p$ reaction, though contributions from that channel with additional photons ($K^+\Lambda p\gamma$, etc.) are also possible. The contributions to the missing mass spectrum for $m_\Sigma+m_N\leq M_X\leq m_\Lambda+m_N+m_\pi$ come from the $pp\to K^+\Lambda p$, $pp\to K^+\Sigma^0p$ and $pp\to K^+\Sigma^+n$ reaction channels and again channels with additional photons. Thus, by subtracting the contribution of $pp\to K^+\Lambda p$ in that invariant-mass region one can extract the sum of the $pp\to K^+\Sigma^0p$ and $pp\to K^+\Sigma^+n$ channels, under the assumption that the reactions with photons provide a negligible contribution. For a reliable estimation of the $pp\to K^+\Lambda p$ contribution it is crucial to know the K^+-meson spectra below the $K\Sigma N$ threshold. Then one can fix the $pp\to K^+\Lambda p$ channel directly from those data and use that result for the extrapolation to the invariant-mass region where the Σ channels are open. As is clear from Fig. 1 in some of the available experiments there are only a few data points below the $K\Sigma N$ threshold. In such a case there is a sizable uncertainty in the data evaluation, which will be reflected, eventually, in the error bars of the corresponding results. This uncertainty is somewhat reduced if there is at least a clean signal of the opening of the $K\Sigma N$ threshold in the spectrum, which is the case for most of the data.

The $pp\to K^+\Sigma^0p$ reaction can be well identified by the detection of the final particles and it has been intensively investigated [26,27]. This information can then be used to deduce the contribution of the $pp\to K^+\Sigma^+n$ channel from the missing mass spectra of inclusive K^+-meson production in the region $m_\Sigma+m_N\leq M_X\leq m_\Lambda+m_N+m_\pi$ for various beam energies. As is obvious from Fig. 1, while some experiments provide information on the K^+-meson momentum spectrum over basically the whole available phase space, this is not the case with others. These limitations again introduce an uncertainty in the data analysis.

For fixing the contribution of the $pp\to K^+\Lambda p$ reaction channel to the missing mass spectrum we utilize Eqs. (3) and (5). Specifically, we determine the reaction amplitude $|\mathcal{A}|$ from the data for $M_X\leq m_\Sigma+m_N$ and use that value for the extrapolation to $M_X\geq m_\Sigma+m_N$. Since it is well known that the Λp final-state interaction (FSI) is sizable [17,18] we take it into account explicitly. This is done by assuming [19,20] that the reaction amplitude $\mathcal{A}$ can be factorized into a practically momentum and energy independent elementary production amplitude $\mathcal{A}_0$ and an FSI factor, $\mathcal{A}_{\Lambda p}$, where the latter is calculated within the Jost-function approach [21]. Details are summarized in Appendix A. As mentioned there, in our analysis we use Jost-function parameters (or equivalently, effective range parameters) from a global fit to the reaction $pp\to K^+\Lambda p$. In principle, one could try to determine those parameters for each data set separately by using the corresponding M_X-spectra [22,23,24]. But then one would require M_X-spectra with rather good mass resolution and statistical accuracy, which is not always the case as seen in Fig. 1 for T_p=2.54 GeV. Consequently, only

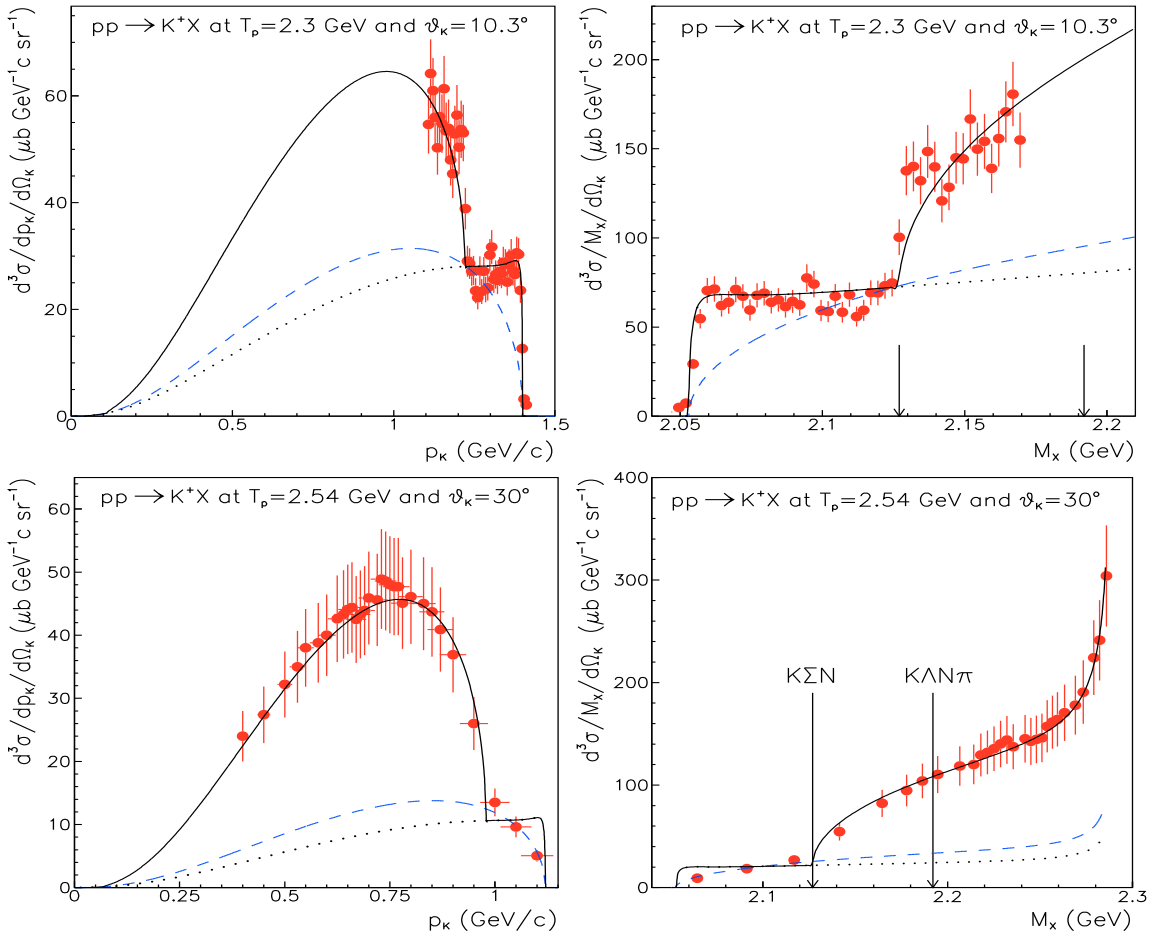

Fig. 1. Left: Experimental information on the K^+-momentum spectra from the $pp \to K^+X$ reaction at T_p=2.3 GeV and θ_K=10.3^o [14] (upper) and at T_p=2.54 GeV and θ_K=30^o [13] (lower). Right: Corresponding missing mass (M_X) spectra obtained by Eq. (5). The arrows indicate the $K\Sigma N$ and $K\Lambda N\pi$ reaction thresholds, respectively. The dotted lines show calculations based on Eqs. (3) and (5) for the $pp \to K^+\Lambda p$ reaction with $|\mathcal{A}_0|$ fitted to the data for $M_X \leq m_\Sigma + m_N$ and Λp FSI effects included via Eq. (8). The dashed lines are result obtained without inclusion of the Λp FSI. The solid lines are the sum of the $pp \to K^+\Lambda p$, $pp \to K^+\Sigma^0 p$ and $pp \to K^+\Sigma^+ n$ cross sections where the sum of the cross sections for the two Σ-hyperon channels was fitted to the data for $m_\Sigma + m_N \leq M_X \leq m_\Lambda + m_N + m_\pi$.

some of the data could be analyzed by including FSI effects that are determined by fitting directly to those data themselves.

Thus, we only fix the elementary production amplitude $\mathcal{A}_0$ by a fit to the corresponding data for $M_X \leq m_\Sigma + m_N$. In practice we determine the constant $|\mathcal{A}_0|$ for each angle and beam energy where experimental K^+ mass spectra are available. Then, by averaging the obtained values for $|\mathcal{A}_0|$ (at a specific energy) over the angular dependence we deduce a result for $\overline{|\mathcal{A}_0|^2}$. The latter quantity can then be compared with the amplitudes deduced from directly measured $pp \to K^+\Lambda p$ cross sections, cf. the discussion in A and the results presented in Sect. 4. This allows us to examine whether the results we extracted from the measured invariant-mass spectra are consistent with the experimental information on the total Λ production cross sections.

Let us now come back to the $pp \to K^+X$ invariant mass spectrum. The dotted lines in Fig. 1 show results of a calculation based on Eqs. (3) and (5) with the FSI included via Eq. (8) and the squared reaction amplitude $|\mathcal{A}_0|$ appropriately adjusted to the spectra at $M_X < m_\Sigma + m_N$. The description of the K^+-meson momentum and missing mass spectra in terms of the contribution from the $pp \to K^+\Lambda p$ reaction looks reasonable. Note that so far we have neglected possible contributions from the reactions with photons in the final state, i.e. $pp \to K^+\Lambda p\gamma$, $pp \to K^+\Lambda p\gamma\gamma$ etc. However, judging from the measurement where a decent number of data points is available for $M_X < m_\Sigma + m_N$, there is not much room for such additional contributions anyway.

In order to estimate the uncertainty that could arise from our treatment of the Λp FSI we consider also an alternative procedure. We perform a fit to the K^+ invariant mass spectrum without FSI, i.e. with pure phase space. But in this case we consider only data points that lie in an energy interval of about 30 MeV from the $K\Sigma N$ threshold downwards for the determination of the reaction amplitude $|\mathcal{A}_0|$ at the various angles and energies. The data points closer to the $K\Lambda N$ threshold exhibit, in general, such obvious FSI effects that it is meaningless to try to fit them with pure phase space. The dashed lines in Fig. 1 show those results obtained without inclusion of the Λp FSI. We will use the predictions of those fits for the $K\Lambda N$ invariant mass spectrum in the region $m_\Sigma + m_N \leq M_X \leq m_\Lambda + m_N + m_\pi$

for extracting the Σ production cross section too. However, we want to emphasize already at this stage that we consider the extrapolation based on the fit that includes the Λp FSI as much more reliable and, therefore, we consider the Σ cross sections deduced from that fit as our definitive results.

Once the contribution from the $pp \to K^+\Lambda p$ channel is established we subtract it from the $pp \to K^+X$ data in the region $m_\Sigma + m_N \leq M_X \leq m_\Lambda + m_N + m_\pi$ in order to obtain the sum of the contributions from the $pp \to K^+\Sigma^0 p$ and $pp \to K^+\Sigma^+ n$ reactions. Possible additional contribution from channels with photons in the final state are again neglected. Utilizing again Eqs. (3) and (5) we determine the corresponding (combined) Σ amplitude $|\mathcal{A}_0|$ for each angle and total energy where experimental K^+ mass spectra are available, etc. However, unlike in the $K^+\Lambda p$ channel, now we do not include an FSI factor in the fitting procedure. Indeed, none of the available data sets exhibits a pronouncend enhancement near the $K\Sigma N$ threshold that would warrant the inclusion of FSI effects. The solid lines in Fig. 1 show the final result, i.e. the contribution from the $pp \to K^+\Lambda p$ reaction plus the fitted contribution from the $pp \to K^+\Sigma N$ channels.

3 Data analysis

In the present paper we analyze the measured K^+-meson momentum spectra published in Refs. [13,14,15]. The achieved results are summarized in Tables 1 and 2. In order to stay as close as possible to physical quantities we do not list the values obtained for the amplitudes $|\mathcal{A}_0|$ but the corresponding cross sections. However, since those amplitudes correspond to data at different angles it is obvious that the given values are not really total cross sections. Rather, they represent cross sections for specific angles, appropriately normalized to the full solid angle. In order to remind the reader on that we put the superscript θ on the corresponding symbols (σ^θ_Λ or σ^θ_Σ).

Comparing the resulting values for σ^θ_Λ and σ^θ_Σ at different angles (at a specific energy) allows conclusions on the angular dependence of the reaction. For facilitating an easy general examination of that dependence we introduce the quantity ξ which is the ratio of σ^θ_Λ and the corresponding (genuine) total cross section σ_Λ obtained from the reference amplitude (16) in conjuction with Eq. (11). Evidently, if there is full consistency between the latter parametrization of the experimental total cross section and the result stemming from our evaluation of the missing mass spectrum then the average of ξ over the kaon angles would amount to unity.

Note that we have neglected the difference between the p and n masses and between the Σ^0 and Σ^+ masses in calculating the excess energies. These are inessential at the high reaction energies we are dealing with here.

As already mentioned, a major source for systematical uncertainties in the data analysis by the method described above is due to the extrapolation of the $K^+\Lambda p$ mass spectrum to the region $m_\Sigma + m_N \leq M_X \leq m_\Lambda + m_N + m_\pi$. It is clear from Fig. 1 that the parametrization including the Λp FSI still differs from the pure phase-space behavior in that region and, therefore, it affects the absolute value of the extracted Σ production cross section. Thus, in order to estimate the uncertainty due to the extrapolation we determine σ^θ_Σ (by a fit based on Eqs. (3) and (5)) for two scenarios: We subtract the contribution from the $pp \to K^+\Lambda p$ (i) including FSI effects as shown by the dotted line in Fig. 1, and (ii) without FSI as given by the dashed line in Fig. 1. Both results for σ^θ_Σ are given in Table 2.

We should mention that even within the Jost-function approach it is not always possible to reproduce the M_X-spectra around the $K^+\Lambda p$ threshold in a perfect way. That might be a problem related to the use of the Jost function formalism or simply due to uncertainties of the parameters α and β (10) used in Eq. (8). In any case, such more subtle aspects of the Λp FSI do not influence the shape of the M_X-spectra above the $K^+\Sigma N$ threshold significantly and are, therefore, not relevant for us.

Let us now discuss the different data sets for the $pp \to K^+X$ reaction one by one. Fig. 2 shows the missing mass spectra from Ref. [14] at the proton beam energy of T_p=2.3 GeV and kaon production angles of θ_K=8.3^o, 10.3^o and 12^o. The dashed lines are the results for the $pp \to K^+\Lambda p$ reaction fitted with a constant reaction amplitude $|\mathcal{A}_0|$ alone, while the dotted lines indicate corresponding results including the Λp FSI.

The M_X-spectra exhibit a substantial enhancement close to the $K^+\Lambda p$ threshold that originates from the Λp FSI. Note that the shape of the near threshold spectra depends somewhat on the K^+-meson production angle and is not reproduced perfectly by using the Jost function (Eq. (8)), especially at the angles θ=8.3^o and 12^o. As was shown in Ref. [22] the M_X-dependence generated by Eq. (8) can be varied by changing the parameters α and β and, in principle, it is possible to achieve a better description of the spectra around the $K^+\Lambda p$ threshold by allowing α and β to depend on the θ_K angle. However, all those variations have only a marginal influence on the description of the missing mass spectra above the $K^+\Sigma N$ threshold, which is the region we are interested in in the present analysis.

The solid lines in Fig. 2 show the sum of the $pp \to K^+\Lambda p$, $pp \to K^+\Sigma^0 p$ and $pp \to K^+\Sigma^+ n$ channels where the contribution of the latter two channels was determined by a fit to the difference between the experimental spectra and the contribution from the $pp \to K^+\Lambda p$ reaction (including FSI effects) via Eqs. (3) and (5). In Tables 1 and 2 we list the corresponding values for σ^θ_Λ and σ^θ_Σ determined from the M_X-spectra for the cases with and without inclusion of the Λp FSI. The quality of the least-square fit can be judged from the given reduced χ^2. As can be seen from the table, there is practically no difference between the results obtained with and without Λp FSI. This is primarily due to the fact that there are sufficient and accurate data on the mass spectrum below the $K\Sigma N$ threshold. Moreover, this threshold is clearly mapped out.

Fig. 3 shows the M_X-spectra from Ref. [15] at the proton beam energy of T_p=2.4 GeV and kaon production angles of θ_K=0^o and 17^o. The notation for the lines are the same as in Fig. 2. Here the $K^+\Sigma N$ threshold is hardly visible in the data, especially at the larger angle, and accordingly there are huge differences in the extracted cross sections between the scenarios with and without Λp FSI, cf. Tables 1 and 2. Ultimately, this is also reflected in the large error bars for the extracted value of σ^θ_Σ. Please recall that the Σ contributions are fitted to the invariant mass spectrum in the range $m_\Sigma + m_N \leq M_X \leq m_\Lambda + m_N + m_\pi$, i.e. between the arrows shown in the fig-

Table 1. Analysis of available data on K^+-meson inclusive momentum spectra from the $pp \to K^+X$ reaction: Results for $pp \to K^+\Lambda p$. Specified are the proton beam energy T_p, the kaon production angle θ_K, and the excess energy ϵ with respect to the Λ-hyperon production threshold. σ^θ_Λ is the $pp \to K^+\Lambda p$ reaction cross section obtained from a fit to the data at a specific angle θ_K, as explained in the text. The factor ξ indicates the angle dependence, cf. text.

Reference	T_p (GeV)	ϵ (MeV)	θ_K (degrees)	w/o Λp FSI	with Λp FSI	
				σ^θ_Λ (μb)	ξ	σ^θ_Λ (μb)
[14]	2.3	252	8.3	23.9±0.7	0.80	24.2±0.9
[14]	2.3	252	10.3	21.3±0.6	0.72	21.8±0.8
[14]	2.3	252	12.0	20.0±0.6	0.68	20.6±0.6
[15]	2.4	285	0	77.0±8.9	2.1	72.9±9.2
[15]	2.4	285	17	52.8±6.7	0.9	31.3±8.1
[13]	2.54	331	20	31.1±3.7	0.55	22.3±2.9
[13]	2.54	331	30	20.5±2.1	0.40	16.2±2.3
[13]	2.54	331	40	24.2±2.3	0.40	16.2±2.7
[14]	2.7	383	12.6	32.7±0.3	0.6	28.0±0.6
[14]	2.7	383	16.1	30.1±0.7	0.55	25.7±0.5
[14]	2.7	383	20	30.3±0.4	0.43	20.1±0.5
[14]	2.7	383	23.5	20.9±0.5	0.4	18.7±0.6
[15]	2.85	431	0	120.3±10.8	1.7	88.0±11.2
[15]	2.85	431	17	39.6±4.8	0.5	25.9±4.2
[15]	2.85	431	32	28.6±6.1	0.5	25.9±5.3

Table 2. Analysis of available data on K^+-meson inclusive momentum spectra from the $pp \to K^+X$ reaction: Results for $pp \to K^+\Sigma N$. Specified are the proton beam energy T_p, the kaon production angle θ_K, and the excess energy ϵ with respect to the Σ-hyperon production threshold. σ^θ_Σ is the sum of the $pp \to K^+\Sigma^0 p$ and $pp \to K^+\Sigma^+ n$ reaction cross sections obtained from a fit to the data at a specific angle θ_K, as explained in the text.

Reference	T_p (GeV)	ϵ (MeV)	θ_K (degrees)	w/o Λp FSI		with Λp FSI	
				σ^θ_Σ (μb)	χ^2/ndf	σ^θ_Σ (μb)	χ^2/ndf
[14]	2.3	178	8.3	13.7±1.0	1.3	14.7±0.9	0.9
[14]	2.3	178	10.3	16.9±1.1	1.5	18.0±1.0	1.6
[14]	2.3	178	12.0	20.0±1.2	1.2	19.5±1.0	2.1
[15]	2.4	211	0	32.5±12.9	0.5	36.1±10.8	0.1
[15]	2.4	211	17	19.0±6.1	0.2	50.6±13.2	1.2
[13]	2.54	257	20	32.0±2.4	0.6	41.4±2.5	0.1
[13]	2.54	257	30	41.0±1.8	0.1	45.7±1.8	0.2
[13]	2.54	257	40	34.2±2.8	3.5	42.4±2.8	0.4
[14]	2.7	309	12.6	37.9±0.8	5.7	47.8±0.5	7.6
[14]	2.7	309	16.1	50.4±1.4	2.9	54.2±1.4	2.6
[14]	2.7	309	20	51.1±0.9	5.5	62.7±0.9	4.2
[14]	2.7	309	23.5	28.4±1.5	1.7	30.6±1.1	1.6
[15]	2.85	357	0	60.1±6.8	1.3	82.5±14.3	0.1
[15]	2.85	357	17	76.7±10.0	0.5	73.4±14.9	0.3
[15]	2.85	357	32	23.4±7.8	2.0	20.0±8.6	0.8

ures, which explains why the corresponding curves are in line with the data in that region but deviate from those at higher M_X values.

Fig. 4 shows the missing mass spectra from Ref. [13] at the proton beam energy of T_p=2.54 GeV and kaon production angles of θ_K=20^o, 30^o and 40^o. There are only few points below the $K^+\Sigma N$ threshold and from those it is hard to see whether there is actually an enhancement due to the Λp FSI. Note that at this specific energy the description of the missing mass spectra for large K^+-meson production angles is very good, in particular, also for the data points above the $K^+\Lambda N\pi$ threshold. Thus, there seems to be not much room for contributions from the reaction channel with an additional pion.

The missing mass spectra from Ref. [14] at the proton beam energy of T_p=2.7 GeV and kaon production angles of θ_K = 12.6^o, 16.1^o, 20^o and 23.5^o are shown in Fig. 5. The data at

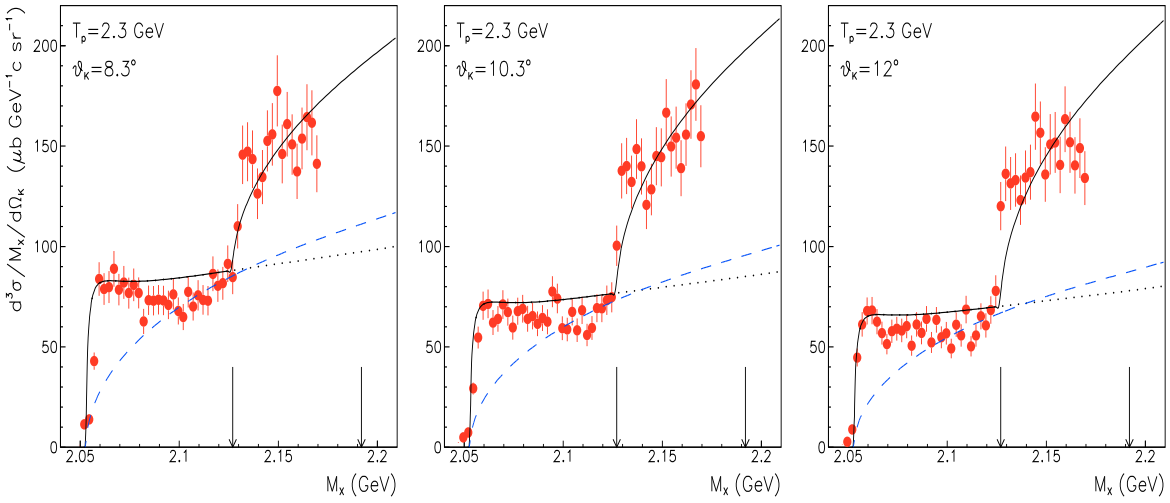

Fig. 2. Experimental missing mass spectra obtained by Eq. (5) from the K^+-meson momentum spectra of the $pp \to K^+X$ reaction [14] at the proton beam energy of T_p=2.3 GeV at different kaon production angles θ_K. The arrows indicate the $K\Sigma N$ and $K\Lambda N\pi$ reaction thresholds, respectively. The dotted lines show calculations based on Eqs. (3) and (5) for the $pp \to K^+\Lambda p$ reaction with $|\mathcal{A}_0|$ fitted to the data for $M_X \leq m_\Sigma + m_N$ and Λp FSI effects included via Eq. (8). The dashed lines are result obtained without inclusion of the Λp FSI. The solid lines are the sum of the $pp \to K^+\Lambda p$, $pp \to K^+\Sigma^0 p$ and $pp \to K^+\Sigma^+ n$ cross sections where the sum of the cross sections for the two Σ-hyperon channels was fitted to the data for $m_\Sigma + m_N \leq M_X \leq m_\Lambda + m_N + m_\pi$.

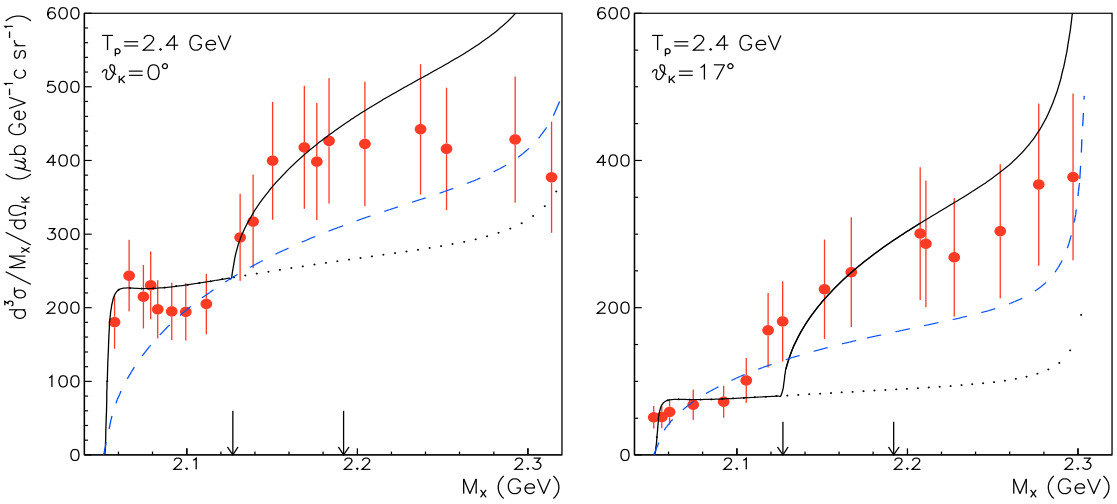

Fig. 3. Experimental missing mass spectra from the $pp \to K^+X$ reaction [15] at the proton beam energy of T_p=2.4 GeV and at different kaon production angles θ_K. Same description of curves as in Fig. 2.

θ_K=12.6^o and θ_K=20^o indicate an enhancement due to the Λp FSI and are well reproduced.

Fig. 6 shows the missing mass spectra from Ref. [15] at the proton beam energy of T_p=2.85 GeV and kaon production angles of θ_K=0^o, 17^o and 32^o. The M_X-spectrum at θ_K=0^o indicates a very strong enhancement due to the Λp FSI. On the other hand, it is somewhat disturbing that there are also data points below the $K^+\Lambda p$ threshold, i.e. outside of the kinematically allowed region. As stated in Ref. [15], this could be due to the momentum resolution of the measurement. In any case, those questionable events do not influence the extraction of the Σ production cross section from the data.

4 Results and discussion

From the results collected in Tables 1 and 2 one can see that the fit to some of the data yielded a rather small χ^2, reflecting the large statistical and systematical uncertainties of the experiments. The fit to the data at T_p=2.7 GeV, on the other hand, leads to a rather large χ^2 because we assume that the missing mass spectra are smooth and, therefore, we cannot describe the large fluctuation of the data for which very small statistical errors are given, as can be seen in Fig. 5.

Let us first comment on the ξ factor, the indicator for the θ_K-angular dependence of the $pp \to K^+\Lambda p$ reaction amplitude. The spectra available at θ_K=0^o indicate a large ξ and, therefore, a strong forward peaking of $|\mathcal{A}_0|$. All other data show

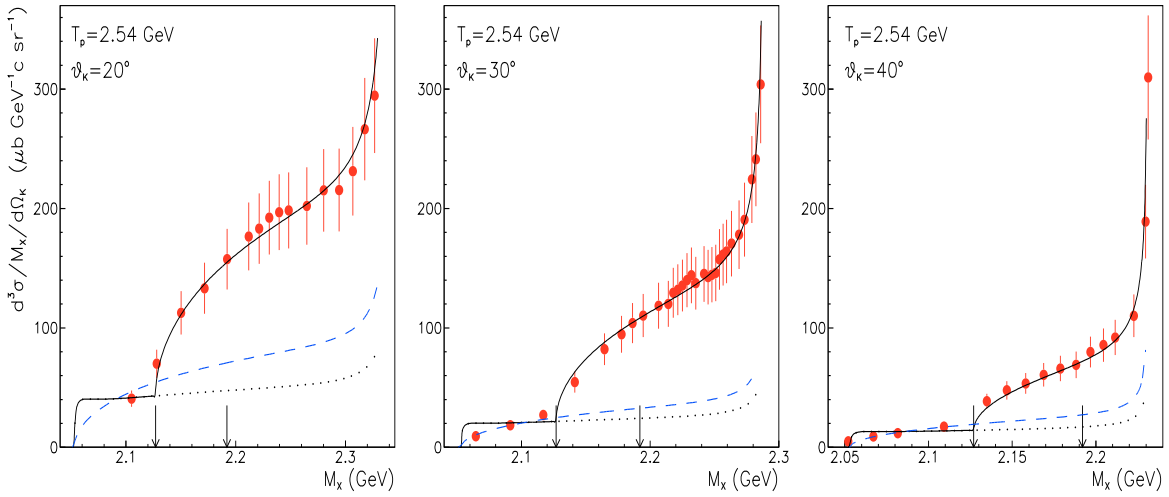

Fig. 4. Experimental missing mass spectra from the $pp \to K^+ X$ reaction [13] at the proton beam energy of T_p=2.54 GeV and at different kaon production angles θ_K. Same description of curves as in Fig. 2.

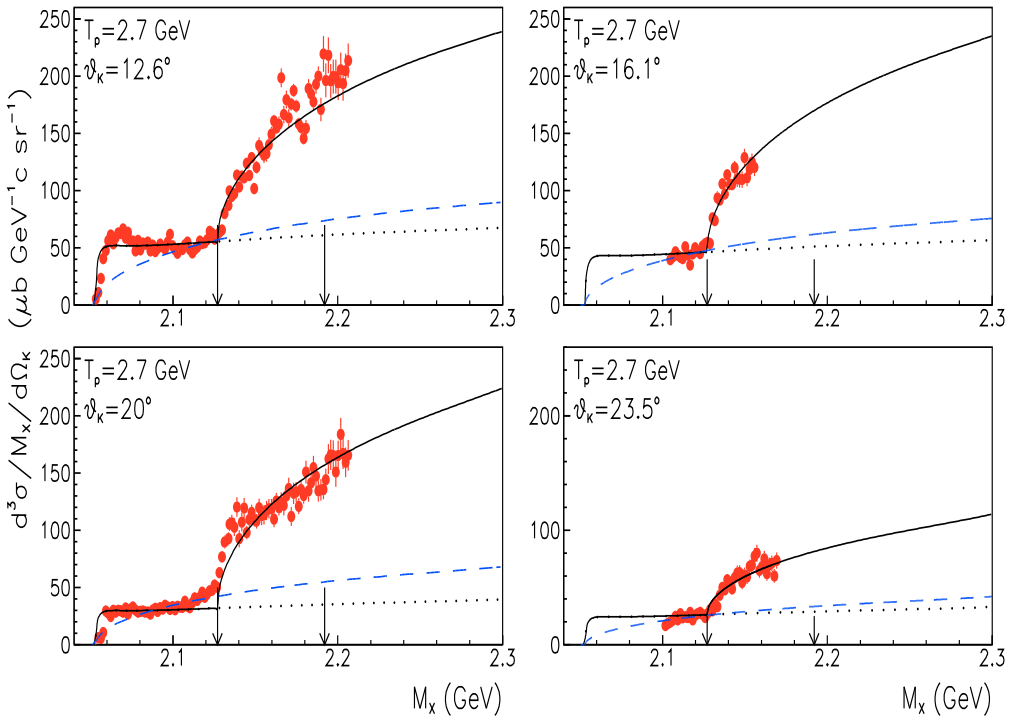

Fig. 5. Experimental missing mass spectra from the $pp \to K^+ X$ reaction [14] at the proton beam energy of T_p=2.7 GeV and different kaon production angles θ_K. Same description of curves as in Fig. 2.

a smooth θ_K-dependence within the range $8.3^o \leq \theta_K \leq 32^o$. In general, for $\theta_K \neq 0^o$ the factor ξ is about $0.4-0.8$ so that the corresponding angle-averaged amplitude is smaller than the reference amplitude for the $pp \to K^+\Lambda p$ reaction computed from Eq. (16), which represents a fit to the measured total reaction cross section. Corresponding results are displayed in the left panel of Fig. 7. We want to point out, however, that for excess energies $170 < \epsilon < 360$ MeV the uncertainty for $\overline{|\mathcal{A}_0|^2}$ as determined directly from available data points from bubble chamber measurements is also in the order of a factor of $\simeq$2, cf. the squares in Fig. 7. Therefore, we conclude that there is a reasonable consistency between the squared reaction amplitudes deduced from the missing mass and the values obtained from direct measurements.

Based on the values for σ_Λ^θ at the same excess energies and for different θ_K from Table 2 we can calculate the mean value and the standard deviation for the $pp \to K^+\Lambda p$ total reaction cross section, cf. Table 3 and the right panel of Fig. 7 (circles). Although for some energies the standard deviations are very large, there is reasonable overall agreement between the results

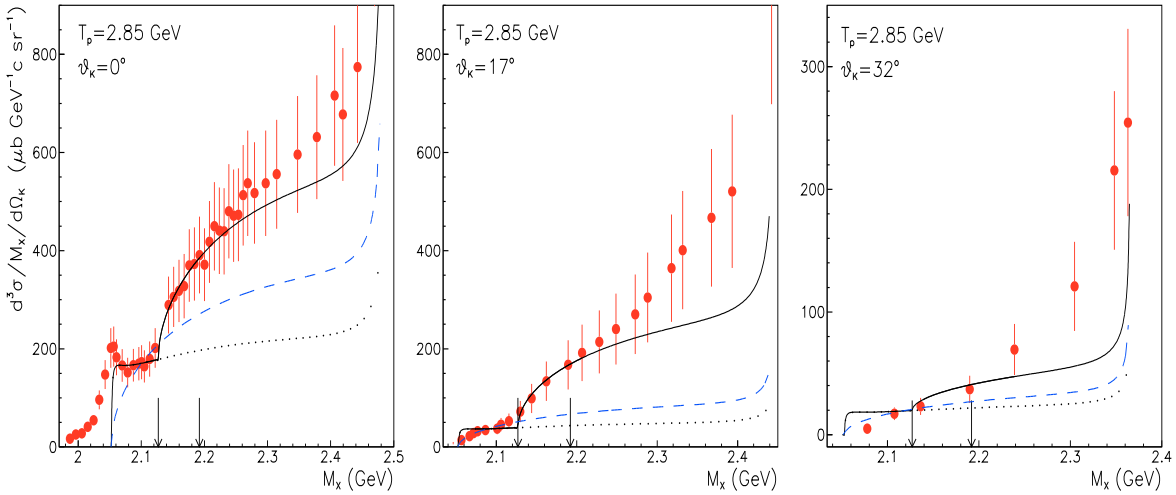

Fig. 6. The same as in Fig. 2 for the proton beam energy of T_p=2.85 GeV. The data are from Ref. [15].

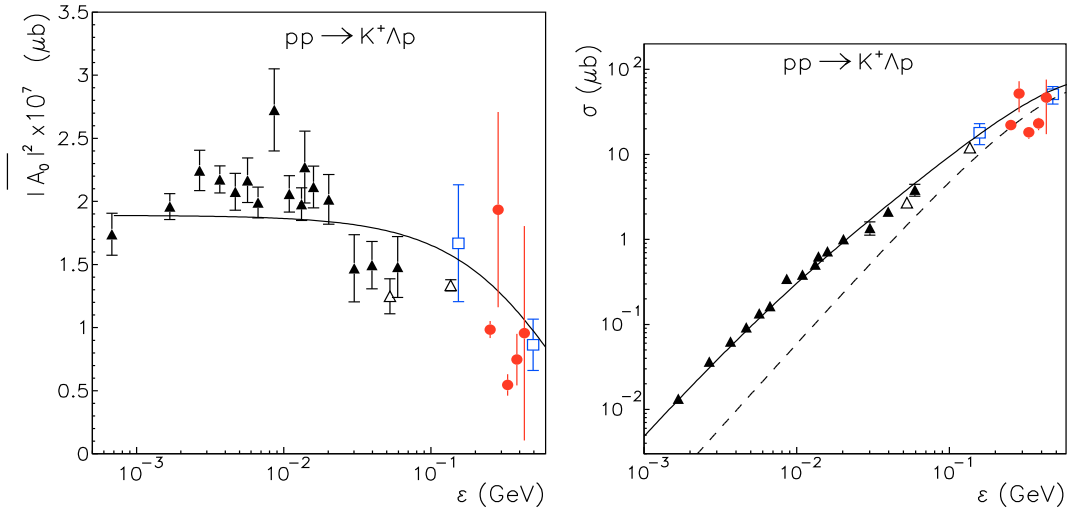

Fig. 7. The $pp \to K^+\Lambda p$ total reaction cross section (right) and corresponding squared reaction amplitude $\overline{|\mathcal{A}_0|^2}$ (left), extracted via Eq. (11), as a function of the excess energy. The solid triangles are data from COSY-11 [25,26,27], the open triangles are from COSY-TOF [28] while the open squares show data taken from Ref. [29]. The dashed and solid lines at the right side show the result of Eq. (11) without (i.e. κ=1) and with Λp FSI, respectively, with $\overline{|\mathcal{A}_0|^2}$ given by Eq. (16). The solid line at the left side shows the parameterization Eq. (16). The circles are results obtained from the missing-mass spectra analysis of the present paper.

extracted from the missing mass spectra and the cross section data from direct measurements.

The sum of the $pp \to K^+\Sigma^0 p$ and $pp \to K^+\Sigma^+ n$ cross sections (σ^θ_Σ), extracted from the missing spectra, shows a more significant angular dependence only at the highest excess energy of ϵ=356.8 MeV, cf. Table 2. For the other energies the dependence of σ^θ_Σ on the K^+-meson production angle is relatively smooth, at least within the uncertainties of the extracted values. From Table 2 one can also see that neglecting the Λp FSI in the extraction procedure yields results for σ^θ_Σ which are, in general, somewhat smaller. But it is reassuring to see that in most of the cases the error bars obtained for the σ^θ_Σ's with and without inclusion of the Λp FSI overlap, indicating that the results are not too sensitive to the specific subtraction prescription. There are only a few cases where there are indeed dramatic differences between the values for the two considered options. As already said, we consider the extrapolation based on the fit that includes the Λp as much more reliable and, therefore, we consider the Σ cross sections deduced from that fit as our definitive results. Averaging over the σ^θ_Σ values extracted at different K^+-meson angles we can now evaluate the Σ production cross section, σ_Σ, and determine the standard deviation for the results obtained from the fit to the M_X-spectra. The corresponding values, for the case where the Λp FSI was taken into account, are listed in Table 4.

In order to deduce the $pp \to K^+\Sigma^+ n$ cross section one needs to subtract from σ_Σ the $pp \to K^+\Sigma^0 p$ cross section. In Fig. 8a we show the existing data for the reaction $pp \to K^+\Sigma^0 p$ as a function of the excess energy. The circles are from the COSY-11 Collaboration [26,27], while the open squares are bubble

Table 3. Results for the total $pp \to K^+\Lambda p$ cross section σ_Λ. The excess energy ϵ is given with respect to the Λ-hyperon production threshold. Our results, extracted from the missing mass spectra, averaged over the θ_K angles, are listed in the upper part of the table. The error bars are computed from the corresponding standard deviation. Experimental results from direct measurements in a comparable energy region and the corresponding references are listed below.

ϵ (MeV)	σ_Λ (μb)	
	our evaluation	missing mass spectrum from Ref.
252	22.2±1.5	[14]
285	52.1±20.8	[15]
331	18.2±2.9	[13]
383	23.1±3.8	[14]
431	46.6±29.3	[15]
	direct measurements	Ref.
138	12.0±0.4	[28]
157	18±5	[39]
431	51±12	[7]

Table 4. Results for the Σ production cross sections. The excess energy ϵ is given with respect to the Σ-hyperon production threshold. σ_Σ is the total Σ production cross section extracted from the missing mass spectra, averaged over the θ_K angles. The error bars are computed from the corresponding standard deviation. The cross section for $\sigma(K^+\Sigma^0p)$ was obtained via Eq. (11), utilizing the parametrization of the cross data for that channel from direct measurements as given in Eq. (6). The cross section for $\sigma(K^+\Sigma^+n)$ is identified with the difference between σ_Σ and $\sigma(K^+\Sigma^0p)$. Listed are also experimental results from direct measurements of the $pp \to K^+\Sigma^0p$ and $pp \to K^+\Sigma^+n$ channels and the corresponding references. Note that $\sigma(K^+\Sigma^0p)$ at $\epsilon = 727.6$ MeV is taken from Ref. [31] and those at 13 and 60 MeV are taken from Refs. [26] (preprint) and [27], respectively.

ϵ (MeV)	σ_Σ (μb)	$\sigma(K^+\Sigma^0p)$ (μb)	$\sigma(K^+\Sigma^+n)$ (μb)	
		our evaluation		missing mass spectrum from Ref.
178	17.7±2.3	4.0±0.3	13.7±2.3	[14]
212	43.4±7.3	5.2±0.5	38.2±7.3	[15]
258	43.2±1.8	6.9±0.7	36.3±1.9	[13]
309	48.8± 11.8	8.9±1.0	39.9±11.8	[14]
357	58.6±27.6	10.6±1.3	48.6±27.6	[15]
		direct measurements		Ref.
13		0.020±0.003	4.56±0.94±2.7	[1]
60		0.482±0.144	44.8±10.7±15.2	[1]
357		13±7	47±13	[7]
728		25±3	48.1±3.5	[8]
849		27±4	85±12	[9]
1006		17^{+4}_{-2}	57±7	[10]
1156		25±3	85±11	[9]

chamber data [29]. Presently there are no experimental results available for $60<\epsilon<360$ MeV, i.e. for the energy range of our analysis. The measurements from the TOF-Collaboration that cover the energy range of our interest are still at the stage of being analysed [30]. Therefore, to proceed further, we fit the $pp \to K^+\Sigma^0p$ total reaction cross section by Eq. (11) with $\kappa=1$, i.e. by neglecting the Σ^0p FSI, and with the appropriate kinematics for the $K^+\Sigma^0p$ channel. The resulting squared reaction amplitude is

$$\overline{|\mathcal{A}_{\Sigma^0}|^2} = (0.61 \pm 0.03) \cdot \exp[(1.34 \pm 0.2)\epsilon] \cdot 10^7 \ \ (\mu\mathrm{b}), \quad (6)$$

with the excess energy given in GeV. Note that the omission of possible Σ^0p FSI effects is in line with the experimental evidence for the $pp \to K^+\Sigma^0p$ channel [26,27] – the available data do not show any visible indication for such a FSI [18,27]. It is also in line with the conclusions we draw from inspecting the experimental mass spectra analysed in the present paper, which likewise exhibit no sign for the presence of a ΣN FSI effects.

The parameterization (6) allows us to calculate the $pp \to K^+\Sigma^0p$ cross section for each of the excess energies, where data on the $pp \to K^+X$ reaction exist. The corresponding values are listed in Table 4. The last column in Table 4 is the difference between σ_Σ and the $pp \to K^+\Sigma^0p$ cross section, which we identify with the $pp \to K^+\Sigma^+n$ cross section. The results are also shown in Fig. 8b (circles). Note that a linear scale is used for displaying the $pp \to K^+\Sigma^+n$ cross section!

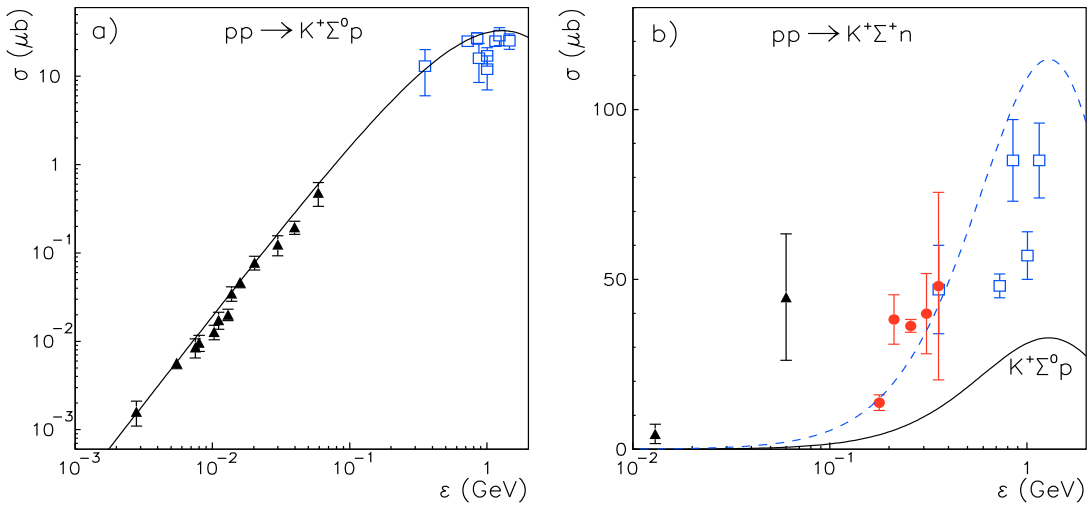

Fig. 8. The $pp \to K^+\Sigma^0p$ (a) and $pp \to K^+\Sigma^+n$ (b) total reaction cross sections as a function of the excess energy. The triangles are data by the COSY-11 collaboration for the $K^+\Sigma^0p$ [26,27] and $K^+\Sigma^+n$ [1] channels, while the squares show bubble chamber data taken from Refs. [7, 8,9,10,29,31]. The circles are results for $pp \to K^+\Sigma^+n$ obtained from our analyis of the missing mass spectra. The solid lines in both panels show the result of Eq. (11) without Σ^0p FSI (i.e. with κ=1) and with $\overline{|\mathcal{A}_{\Sigma^0}|^2}$ given by Eq. (6). The dashed line in (b) is the same as the solid line, but multiplied by a factor 3.5.

First let us compare our results with the bubble chamber data [7,8,9,10] shown by the open squares in Fig. 8b and listed also in Table 4. The $pp \to K^+\Sigma^+n$ cross section of 47±13 μb at ϵ=357 MeV was measured by Louttit et al. [7] and it is in agreement with our result at the same energy, cf. Table 4 – though, unfortunately, at this highest energy of our analysis there is a large uncertainty due to the angular dependence of the extracted cross section as can be seen from Table 2. The $pp \to K^+\Sigma^+n$ data [8,9,10] at higher energies indicate large fluctuations. We want to remark that the two points at $\epsilon \simeq$ 0.85 and 1.1 GeV represent the largest reported cross sections with 85 μb (at both energies) and are available [9] only in an UCLA preprint. For the lowest energy where missing mass spectra are available, ϵ=178 MeV, we deduced a cross section of 13.7±2.3 μb from the data. There are two so far unpublished measurements of the $pp \to K^+\Sigma^+n$ cross section by the TOF collaboration at somewhat lower energy, i.e. at beam momenta of 2.06 GeV (ϵ=98 MeV) [32] and 2.157 GeV (ϵ=128 MeV) [33], respectively. It is worth mentioning that their results are roughly in line with the value we obtained. The results from the COSY-11 Collaboration at low excess energies have been available only recently [1]. Their $pp \to K^+\Sigma^+n$ cross section of 44.8±10.7±15.2 at ϵ=60 MeV is as large as those at high energies, cf. Table 4 and Fig. 8.

For illustration purposes we include the result for the $pp \to K^+\Sigma^0p$ cross section also in Fig. 8b (solid line). The dashed line shows the same cross section, but multiplied by a factor 3.5. Obviously its energy dependence is very different from that exhibited by the $pp \to K^+\Sigma^+n$ cross section if one considers *all* available data. However, it is interesting to see that the curve would be roughly in line with the trend of the $K^+\Sigma^+n$ data, including the ones obtained from our analysis, if one disregards the COSY-11 events and the measurements from Refs. [8,10]. The data from the last two references are in clear contradiction to the results from Ref. [9] anyway. On the other hand, one has to keep in mind that the latter data were never officially published.

Provided that all data are indeed correct, it will be difficult to find plausible explanations for the drastically different behavior of the $pp \to K^+\Sigma^+n$ cross section. The model calculations [2,3,4,5,6] available for this reaction channel indicate that the energy dependence of the cross section is similar to the one of $pp \to K^+\Sigma^0p$. After all, the energy dependence is to a considerable part determined simply by phase-space factors. Evidently, the model predictions [2,3,4,5] disagree strongly with the new data [1] of the COSY-11 Collaboration. Since those calculations describe the $pp \to K^+\Sigma^+n$, $pp \to K^+\Sigma^0p$ and $pp \to K^0\Sigma^+p$ reactions with the same dynamical input, additional mechanisms can be introduced only by assuming that they contribute to the $pp \to K^+\Sigma^+n$ channel alone. But not even a recent study that focusses on the $pp \to K^+\Sigma^+n$ reaction only and invokes contributions from the $\Delta(1620)$ resonance is able to describe the COSY-11 data satisfactorily [6]. Of course, possible additional contributions could arise from the excitation of crypto-exotic baryons, as was speculated in Ref. [1], that then decay into the $K\Sigma$ channel. Such crypto-exotic baryons were discussed [34] recently in the context of the new ANKE-COSY results [35] on ϕ-meson production. An indication for a possible crypto-exotic baryon was also reported in Ref. [36], based on an analysis of the Σ^0K^+ invariant mass spectrum.

Anyway, instead of embarking on further speculations we believe that it would be more instructive to perform new measurements of the $pp \to K^+\Sigma^+n$ reaction in the near-threshold region. The method used in the present paper can be also applied in the analysis of data that can be taken at ANKE [37] and HIRES [38] at COSY. These experimental facilities are perfectly suited for obtaining K^+-meson spectra with high statistics and high resolution. Such exeriments would also allow to

shed light on the angular dependence of the reaction amplitude, which we expect to be very weak at low excess energies.

5 Summary

In the present paper we determined the sum of the $pp \to K^+\Sigma^+n$ and $pp \to K^+\Sigma^0p$ cross sections from inclusive K^+-meson momentum spectra in the energy range T_p = 2.3 - 2.85 GeV, available in the literature. We showed that, after transformation of the momentum spectrum to the missing mass (M_X) spectrum, the contribution from the reaction channels with Λ and Σ hyperons can be isolated by inspecting the data between the $K^+\Lambda p$, $K^+\Sigma N$, and $K^+\Lambda N\pi$ thresholds and we demonstrated that the M_X-spectra can be well described when taking into account the contributions from the $pp \to K^+\Lambda p$, $pp \to K^+\Sigma^+n$ and $pp \to K^+\Sigma^0p$ reactions. The angular dependence of the reaction amplitude was accounted for by fitting the K^+-meson spectra at different angles. Total cross sections were then deduced by averaging over the angles.

As a test we first determined the $pp \to K^+\Lambda p$ cross sections at those excess energies where the invariant mass spectra are availabe. It turned out that the cross sections extracted by us are roughly in line with results from direct measurements in the same energy region.

Utilizing available information on the $pp \to K^+\Sigma^0p$ cross section, we then deduced total cross sections for the $pp \to K^+\Sigma^+n$ channel. The obtained results were discussed and compared with existing data from direct measurements. At the specific energy T_p = 2.85 GeV there is also a data point from a bubble chamber measurement [7] and it was reassuring to see that our result is compatible with that experiment. The cross section obtained for T_p = 2.3 GeV is with 13.7 ± 2.3 μb considerably smaller than the value found in a recent experiment by the COSY-11 Collaboration at a somewhat lower beam energy Thus, our new cross section values, together with the already available data, indicate that the energy dependence of the cross section for the reaction $pp \to K^+\Sigma^+n$ could differ drastically from that of the $pp \to K^+\Sigma^0p$ channel. This would be certainly rather surprising. Apparently, further experiments are necessary to confirm this unusual behaviour. If such experiments indeed corroborate the present findings then it is likely that peculiar and potentially exotic mechanisms play a role in the reaction $pp \to K^+\Sigma^+n$.

Acknowledgments

This work was partially supported by Deutsche Forschungsgemeinschaft through funds provided to the SFB/TR 16 "Subnuclear Structure of Matter". This research is part of the EU Integrated Infrastructure Initiative Hadron Physics Project under contract number RII3-CT-2004-506078. A.S. acknowledges support by the COSY FFE grant No. 41760632 (COSY-085) and the JLab grant SURA-06-C0452.

A Treatment of the final-state interaction

In the present work we take into account effects of the final-state interaction in the Λp channel. Following standard arguments [19,20] we assume that the reaction amplitude $\mathcal{A}$ can be factorized into a practically momentum and energy independent elementary production amplitude $\mathcal{A}_0$ and an FSI factor:

$$\mathcal{A} \approx \mathcal{A}_0 \times \mathcal{A}_{\Lambda p} \, . \tag{7}$$

The FSI effects are then taken into acount within the Jost function approach

$$|\mathcal{A}_{\Lambda p}|^2 \approx \frac{q^2+\alpha^2}{q^2+\beta^2} \, , \tag{8}$$

where the momentum q is given by

$$q = \frac{\lambda^{1/2}(s_Q, m_\Lambda^2, m_p^2)}{2\sqrt{s_Q}} \, , \tag{9}$$

and the parameters α and β were taken as

$$\alpha = -72.3 \text{ MeV} \, , \quad \beta = 212.7 \text{ MeV}. \tag{10}$$

These parameters are related to the scattering length a and effective range r of the Λp interaction [17]. To be specific, they correspond to the values a = -1.8 fm and r = 2.8 fm. The parameters of the Λp FSI that we use here were obtained in Refs. [17, 18] from a global phenomenological analysis of all available data on the reaction $pp \to K^+\Lambda p$. But, one should keep in mind that the scattering parameters are not fixed uniquely. Actually, we have shown in Ref. [17] that a large set of different values for the scattering length a and effective range r allows to reproduce the energy dependence of the $pp \to K^+\Lambda p$ cross section data. Some of these parameters coincide with results predicted by modern YN models [40,41,42,43,44].

Based on Eqs. (7-8) one can then write the total reaction cross section for the reaction $pp \to K^+\Lambda p$ in the form [17]

$$\sigma_\Lambda(\epsilon) = \frac{\Phi_3}{2^6\pi^5\lambda^{1/2}(s, m_p^2, m_p^2)} \; \overline{|\mathcal{A}_0|^2} \; \kappa(\epsilon) \, . \tag{11}$$

Here $\overline{|\mathcal{A}_0|^2}$ is the (angle) averaged reaction amplitude squared while κ is a factor that represents the FSI effects. The 3-body phase space is

$$\Phi_3 = \frac{\pi^2}{4s} \int\limits_{(m_\Lambda+m_p)^2}^{(\sqrt{s}-m_K)^2} \lambda^{1/2}(s, s_Q, m_K^2) \times \lambda^{1/2}(s_Q, m_\Lambda^2, m_p^2) \, \frac{ds_Q}{s_Q} \, . \tag{12}$$

In the nonrelativistic limit it reduces to

$$\Phi_3 \to \frac{1}{2^7\pi^2} \, \frac{\sqrt{m_K m_\Lambda m_p}}{(m_K+m_\Lambda+m_p)^{3/2}} \; \epsilon^2 \, . \tag{13}$$

The non-relativistic form is a good approximation for the $pp \to K^+\Lambda p$ reaction up to excess energies of $\epsilon \simeq 1$ GeV and we use it in the present investigation. Also, in this case the factor κ can be computed analytically for the Jost function approach (8), and under the assumption that there is only a FSI in the Λp system [17]. It amounts to

$$\kappa(\epsilon) = 1 + \frac{4\beta^2 - 4\alpha^2}{(-\alpha + \sqrt{\alpha^2 + 2\mu\epsilon})^2} \, , \tag{14}$$

where μ stands for the reduced mass

$$\mu = \frac{m_\Lambda m_p}{m_\Lambda + m_p} \, , \tag{15}$$

and the parameters α and β for the Λp FSI given by Eq. (10). Note that $\kappa \equiv 1$ in case that FSI effects are neglected.

The $pp \to K^+\Lambda p$ reaction can be directly identified through the detection of the final particles and, therefore, there are already many precise cross section data available in the literature [25,26,27,28,29]. These data, displayed in Fig. 7 (right side), allow a straight-forward determination of the squared reaction amplitude $\overline{|\mathcal{A}_0|^2}$ by means of Eq. (11). Corresponding results are shown in Fig. 7 on the left hand side. For our purposes it is also convenient to parametrize the experimental cross section by means of a simple function. This is achieved with

$$\overline{|\mathcal{A}_0|^2} = (1.89 \pm 0.04) \cdot \exp[(1.34 \pm 0.1)\,\epsilon] \cdot 10^7 \;\; (\mu\mathrm{b}) \, , \tag{16}$$

where the parameters were determined by a fit to the data in Fig. 7 for energies ϵ<500 MeV. Here ϵ is the excess energy in GeV. The corresponding curve, including also the Λp FSI via Eq. (14), is shown by the solid line in Fig. 7.

References

1. T. Rozek *et al.*, Phys. Lett. B **643**, 251 (2006) [arXiv: nucl-ex/0607034].
2. J.M. Laget, Phys. Lett. B **259**, 24 (1991).
3. A. Sibirtsev, K. Tsushima, W. Cassing, A.W. Thomas A W, Nucl. Phys. A **646**, 427 (1999) [arXiv: nucl-th/9810070].
4. K. Tsushima, A. Sibirtsev, A.W. Thomas, Phys. Rev. C **59**, 369 (2000) [arXiv: nucl-th/9801063].
5. R. Shyam, Phys. Rev. C **73**, 035211 (2006) [arXiv: nucl-th/0512007].
6. J.J. Xie, B.S. Zou, arXiv: nucl-th/0701021.
7. R.I. Louttit *et al.*, Phys. Rev. **123**, 1465 (1961).
8. I. Sondhi *et al.* Phys. Lett. B **26**, 645 (1968).
9. W.M. Dunwoodie *UCLA Report No. UCLA-1033* (1968) unpublished.
10. W. Chinowsky *et al.* Phys. Rev. **165**, 1466 (1968).
11. A. Gillitzer, D. Grzonka, Int. J. Mod. Phys. A **20**, 539 (2005).
12. H.H. Adam *et al.*, arXiv: nucl-ex/0411038.
13. W.J. Hogan, P.A. Piroue, J.S. Smith, Phys. Rev. **166**, 1472 (1968).
14. R. Siebert *et al.*, Nucl. Phys. A **567**, 819 (1994).
15. J.T. Reed *et al.*, Phys. Rev. **168**, 1495 (1968).
16. E. Byckling, K. Kajantie, *Particle Kinematics* Willey and Sons, New York (1973).
17. A. Sibirtsev, J. Haidenbauer, H.-W. Hammer, S. Krewald, Eur. Phys. J. A **27**, 269 (2006) [arXiv: nucl-th/0512059].
18. A. Sibirtsev, J. Haidenbauer, H.-W.Hammer, U.-G. Meißner, Eur. Phys. J. A **29**, 363 (2006) [arXiv: hep-ph/0608098].
19. K. Watson, Phys.Rev. **88**, 1163 (1952).
20. A.B. Migdal, Sov. Phys. JETP **1**, 2 (1955).
21. M. Goldberger, K.M. Watson, *Collision Theory* Willey, New York. (1964).
22. F. Hinterberger, A. Sibirtsev, Eur. Phys. J. A **21**, 313 (2004) [arXiv: nucl-ex/0402021].
23. A. Gasparyan, J. Haidenbauer, C. Hanhart, J. Speth, Phys. Rev. C **69**, 034006 (2004) [arXiv: hep-ph/0311116].
24. A. Gasparyan, J. Haidenbauer, C. Hanhart, Phys. Rev. C **72**, 034006 (2005) [arXiv: nucl-th/0506067].
25. J.T. Balewski *et al.*, Phys. Lett. B **420**, 211 (1998) [arXiv: nucl-ex/9803003].
26. S. Sewerin *et al.*, Phys. Rev. Lett. **83**, 682 (1999). [arXiv: nucl-ex/9811004].
27. P. Kowina *et al.*, Eur. Phys. J. A **22**, 293 (2004) [arXiv: nucl-ex/0402008].
28. R. Bilger *et al.*, Phys. Lett. B **420**, 217 1998
29. A. Baldini, V. Flaminio, W.G. Moorhead, D.R.O. Morrison, *Landolt-Börnstein New Series* **12**, 149 (1998).
30. TOF-COSY Collaboration, *private communication*
31. E. Bierman, A.P. Colleraine, U. Nauenberg, Phys. Rev. **147**, 922 (1966).
32. P. Schönmeier, *PhD thesis, Technical University of Dresden, Germany* (2003) unpublished.
33. L. Karsch, *PhD thesis, Technical University of Dresden, Germany* (2005) unpublished.
34. A. Sibirtsev, J. Haidenbauer, Ulf-G. Meißner, Eur. Phys. J. A **27**, 263 (2006). [arXiv: nucl-th/0512055].
35. M. Hartmann *et al.*, Phys. Rev. Lett. **96**, 242301 (2006) [arXiv: hep-ex/0604010].
36. Yu.M. Antipov *et al.*, Phys. Atom. Nucl. **65**, 2070 (2002).
37. S. Barsov *et al.*, Nucl. Instr. Meth. A **462**, 364 (2001)
38. F. Hinterberger, S.N. Nedev, R. Siudak, Int. J. Mod. Phys. A **20** 291 (2005).
39. W.J. Fickinger, E. Pickup, D.K. Robinson, E.O. Salant, Phys. Rev. **125**, 2082 (1962).
40. T.A. Rijken, V.G.J. Stoks, Y. Yamamoto, Phys. Rev. C **59**, 21 (1999) [arXiv: nucl-th/9807082].
41. H.-W. Hammer, Nucl. Phys. A **705**, 173 (2002) [arXiv: nucl-th/0110031].
42. J. Haidenbauer, Ulf-G. Meißner, Phys. Rev. C **72**, 044005 (2005) [arXiv: nucl-th/0506019].
43. H. Polinder, J. Haidenbauer, Ulf-G. Meißner Ulf-G Nucl. Phys. A **779**, 244 (2006) [arXiv: nucl-th/0605050].
44. T. A. Rijken, Y. Yamamoto, Phys. Rev. C **73**, 044008 (2006) [arXiv: nucl-th/0603042].